AN APPARATUS FOR THE STUDY OF ELECTRON DETACHMENT PROCESSES IN NEGATIVE ION – ATOM AND MOLECULE COLLISIONS

T. J. Kvale[1] and D. G. Seely[2]

[1] *Department of Physics and Astronomy, University of Toledo, Toledo, Ohio 43606 USA*

[2] *Department of Physics, Albion College, Albion, Michigan 49224 USA*

1. SUMMARY

This paper summarizes the main features of an apparatus constructed at the University of Toledo for the study of various scattering processes in intermediate energy, ion – atom collisions. The main purpose of this facility is to provide experimental data which serve as benchmarks to test current scattering theories for those processes. Recent measurements of single electron detachment (SED) and double electron detachment (DED) total cross sections for 5–50 keV H^- ions incident on noble gases and for 10–50 keV H^- ions incident on CH_4 molecules were conducted in this laboratory. As a result of an analysis of the scattered beam growth curves, information about other charge–changing cross sections in the hydrogen–atom (molecule) collision systems were obtained, as well.

2. INTRODUCTION

The detachment of electron(s) from negative ions in intermediate-energy collisions with atomic gases is an important component of understanding the more general subject of charge–changing processes in ion – atom collisions. These relatively large detachment cross sections also result in negative ions being efficient electron donors in variety of practical applications. Because of these basic physics and applied physics interests, an apparatus was

Proceedings of the Symposium on Recent Advances in Mechanics, Honorary Volume for Prof. D.D. Raftopoulos, E.E. Gdoutos, ed., Democritus University of Thrace, Xanthi, Greece, July 1998

DISCLAIMER

constructed at the University of Toledo to study electron detachment in ion – atom collisions. The projectile ion was chosen to be the fundamental negative ion, H^-, consisting of one proton and two electrons, so that the physics of the interaction would not be obscured with approximations inherent in many-electron ions. The choice of H^- also governed the design parameters of the ion source section of the apparatus and the choice of intermediate-energy, ion - atom collisions governed the size, type of detectors, apparatus configuration, and other design parameters of the facility. In this paper, we summarize the important apparatus features and other various experimental details by which we have obtained the cross sections which were reported in earlier papers [1-5].

3. EXPERIMENTAL APPARATUS

An overview of the apparatus used in the electron detachment measurements is shown schematically in Figure 1. Briefly, the facility consists of: a d.c. negative ion accelerator; a scattering chamber containing a gas target cell; a charge–state analyzing magnet; three scattered–beam detectors; and associated electronics. The apparatus is approximately 5 m long from the ion source to the scattered beam detectors. All beamline sections of the apparatus were maintained at a vacuum of 10^{-6} Torr, or better.

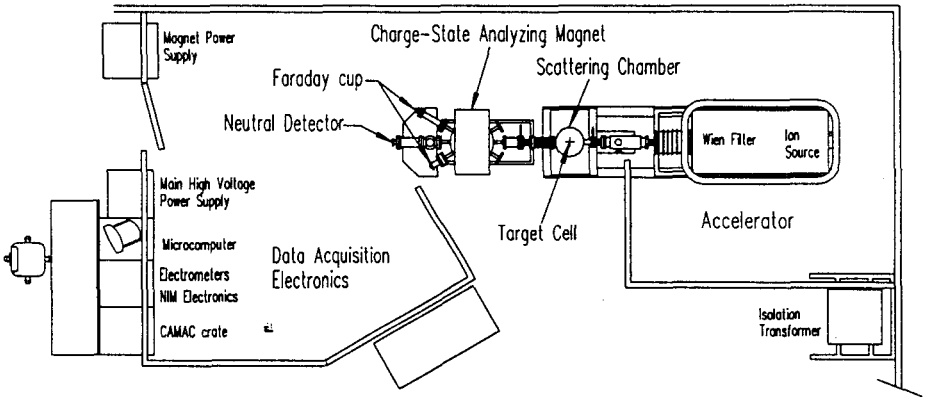

Figure 1. An Overview Drawing of the UT-Negative Ion Accelerator Facility

3.1 Accelerator & Negative Ion Beam Formation

The formation of the projectile negative ion beam occurred in the beamline

components shown in Figure 2. Negative ions were created in a commercial duoplasmatron ion source located inside the accelerator terminal. A fixed potential difference of typically +5kV was applied across the source aperture and the Extractor electrode to extract negative ions from the plasma in the ion source. The ions then entered a three-element, coaxial, tubular electrostatic ion optics lens (Einzel Lens) which was used to form and focus the extracted ions into an ion beam. After the Einzel Lens, the ions then entered an instrument (Wien Filter) which contained crossed magnetic and electric fields. The kinematics of this device were such that only ions having the correct momentum would pass through the device undeflected. The fields were adjusted so that the Wien Filter operated as a mass–analyzer which selected only the $^1H^-$ ion component of the extracted beam coming from the ion source. A calibrated, 0– to 50–kV power supply was connected to the accelerator terminal and was adjusted to accelerate the H^- ions to the desired collisional kinetic energy.

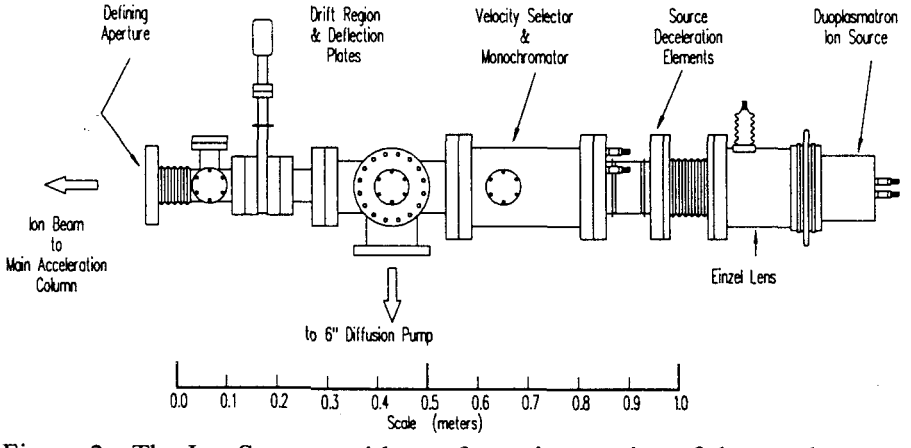

Figure 2. The Ion Source and beam formation section of the accelerator

3.2 Target Cell

After exiting from the acceleration column, the fast H^- ions were directed into a target cell (shown in Figure 3) located inside the scattering chamber vacuum housing. The H^- ion beam was initially collimated by the 2.0 mm diameter acceleration column entrance aperture and the 1.0 mm diameter target cell entrance aperture, which were separated by a distance of 1.4 m. Two 0.5 mm wide crossed slits were then placed in the ion beam path prior

to the scattering chamber housing to further define the incident H^- ion beam.

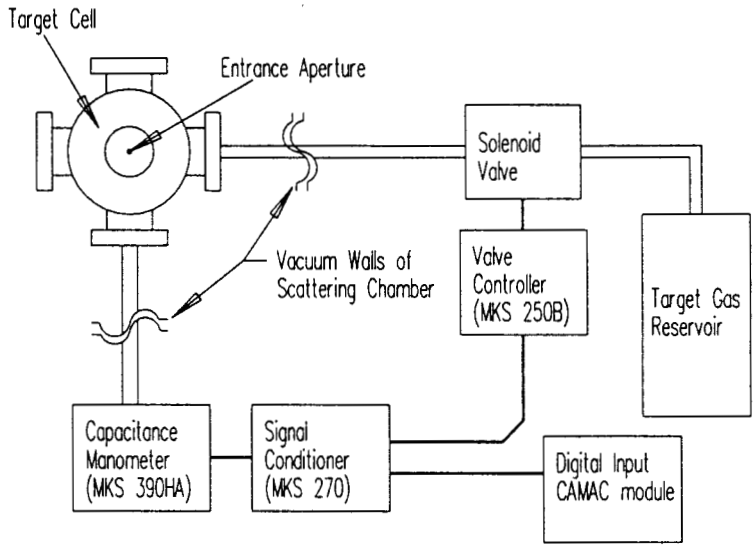

Figure 3. The Target Cell and associated pressure control system

The gas target cell was a modified, stainless steel, four–way, 1.33 in. knife-edge, metal-gasket–type cross. The H^- ions entered the target cell through a 1.0 mm diameter beveled aperture and exit the target cell through a 1.2 mm diameter beveled aperture. The entrance and exit apertures were separated by a distance of 3.10 cm. Research grade atomic or molecular gas was admitted into the target cell through a solenoid valve connected to one arm of the target cell by 1/4 in. diameter stainless steel tubing. The gas pressure inside the target cell was measured by a calibrated capacitance manometer connected to a different arm of the target cell through 1/4 in. diameter stainless steel tubing. The remaining two arms of the target cell were vacuum sealed. The pressure in the surrounding vacuum chamber was maintained at a vacuum of 10^{-6} Torr, or better, by a six inch diffusion pump even when the target cell was in operation.

3.3 CHARGE-STATE ANALYZING MAGNET

After the incident beam passed through the target cell, the fast, scattered beam entered the zero–degree, beam–entrance port of a charge–state analyzing magnet shown in Figure 4. This magnet provided the charge–state

analysis of the scattered ion beam. The magnetic field was adjusted to

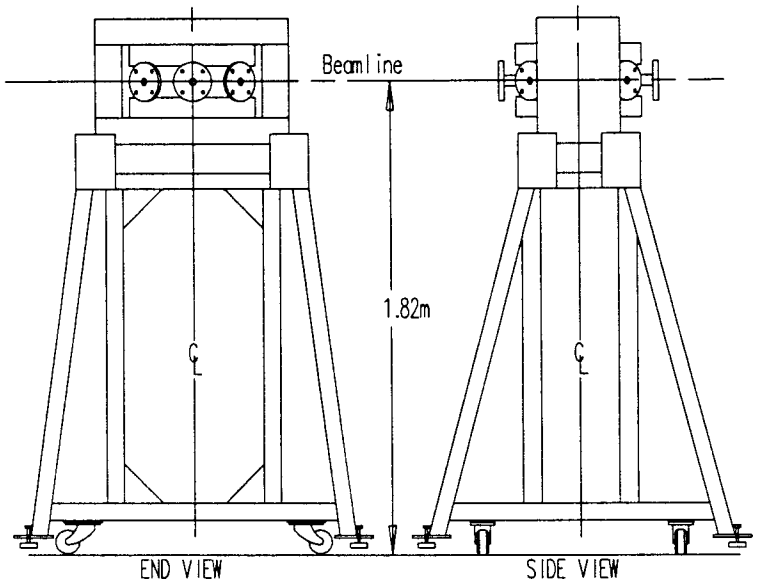

Figure 4. The Charge-state analyzing magnet and support structure

deflect the H^- and H^+ ion components into ±30° beam exit ports, whereas the H^0 atoms passed undeflected through the magnet and entered the neutral detector connected to the zero–degree beam–exit port of the magnet. This beam separation allowed each charge–state component of the scattered beam to be simultaneously detected by separate detectors for each of the three charge–state beams. This simultaneous detection of all three scattered beams has the distinct advantage of allowing both single electron detachment and double electron detachment total cross sections to be determined absolutely *in situ* without having to rely on other experiments and/or theoretical models.

3.4 PARTICLE BEAM DETECTORS

Two different types of detectors were needed in the detection of the three scattered beams, since two of the beams were of charged particles (H^- and H^+) while the third beam was electrically neutral (H^0). The conversion of the neutral H^0 atom current to an electrical signal was based on the principle of the secondary emission of electrons (and negative ions) arising from the impact of an energetic H^0 atom beam on a metal surface. The neutral

detector construction and operation have described in a separate paper [4], so only a synopsis of it is included here for continuity. The inner shield of the neutral detector (shown in Figure 5) was biased at a positive voltage (10–50 V) relative to ground. This voltage attracted the secondary negative particles (secondary emission coefficient or yield) away from the copper cylinder where the H° atoms struck and resulted in a net positive current to the copper cylinder. This positive current is identified as the neutral detector current S_0. The secondary emission coefficient γ was determined from the closure relation ($F_{-1} + F_0 + F_1 = 1$, where F is defined in Section 4) since all three scattered beam components (H^-, H^0, and H^+) were simultaneously measured in this experiment. The accurate determination of γ is crucial to the absolute measurements of single electron detachment measurements. The method of determining γ is provided in detail in Reference 1.

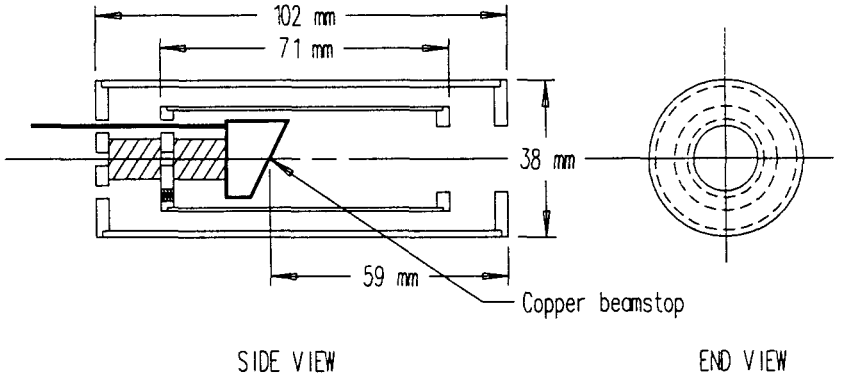

Figure 5. Schematic Drawing of the Neutral H° Detector

The H^- ions exiting the charge–state analyzing magnet were deflected into a shielded Faraday cup attached to one of the 30° exit ports. The protons, resulting from double detachment collisions, were deflected into a similar shielded Faraday cup attached to the other 30° exit port. The Faraday cup construction is shown in Figure 6. The Faraday cup shields were biased at a negative voltage ($\geq$ 50 V) relative to ground potential to suppress the secondary electrons and negative ions emitted when the fast ions strike the inner conductors of the Faraday cups. Both Faraday cup currents and the neutral current were measured by separate, calibrated electrometers. The

uniformity of the detector sensitivity was crucial in the quality of the data

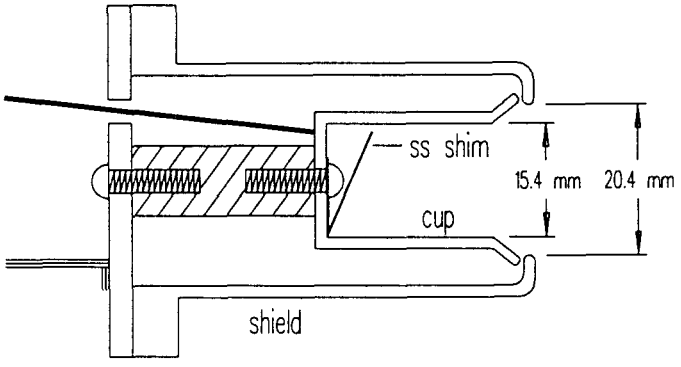

Figure 6. Schematic drawing of the H^- and H^+ beam Faraday Cup detectors.

from the apparatus. Figure 7 shows the detected Faraday cup current as the H^- ion beam was swept across the face of the detector by the adjustment of the magnetic field of the charge-state analyzing magnet. The two signal peaks were caused by the H^- ion beam striking the outer shields of the Faraday cup and liberating additional electrons from those surfaces similar to what was described earlier in the neutral detector operation. These electrons were accelerated to the center beamstop by the electric field applied in that region of the Faraday cup. These electrons added to the negative current signal from the H^- beam, resulting in the increased negative electrical current shown as peaks in Figure 7. However, when the H^- ion beam was directed at the beamstop inside the Faraday cup, the detection sensitivity was very uniform as evidenced by the essentially flat signal in between the peaks as shown in Figure 7.

The measured H^- and H^+ ion currents, as well as the corresponding neutral detector current, S_0, and target gas pressure, P, were automatically and/or manually input into the microcomputer. After a complete set of growth curve data was acquired, the data acquisition program was terminated and the datafile was stored for later input into a separate analysis program for determination of the resulting cross sections.

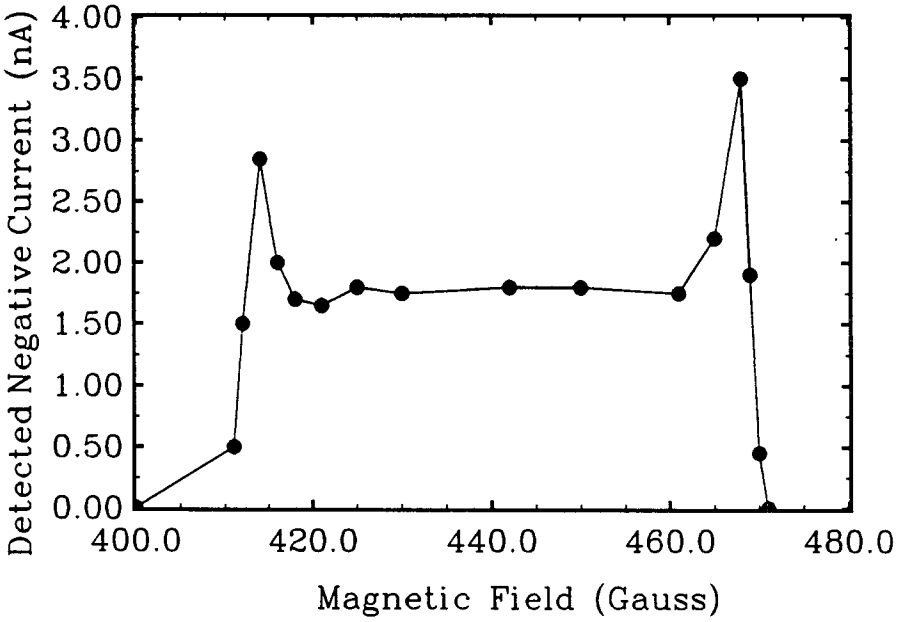

Figure 7. The negative current measured on the H^- Faraday cup as a function of the magnetic field of the charge-state analyzing magnet.

4. SCATTERED BEAM FRACTIONS

Because of the prominence of the detachment processes, significant projectile partial beams of the other hydrogen charge states (H° and H^+) are present and can interact with the target gas atoms. The charge–state composition of the incident H^- ion beam evolves as it passes through the target gas due to charge–changing collisions with the target atoms, as shown schematically in Figure 8. The target thickness, π, is defined by $\pi = nl$, where n is the target gas atom density, and l is the distance (scattering or interaction length) the beam has traversed in the gas. For a fixed H^- ion impact energy, the beam–attenuation curve for the negative–ion current, $I_{-1}(\pi)$, and the beam–growth curves for the proton current, $I_1(\pi)$, and the neutral detector current, $S_0(\pi)$, were obtained by measuring these currents as a function of the target thickness. The target thickness ranged from $\pi = 0$ to 3×10^{14} molecules/cm^2 by changing the target gas pressure in the target cell. The target gas density, n, is obtained from the ideal gas law and the target gas pressure and temperature.

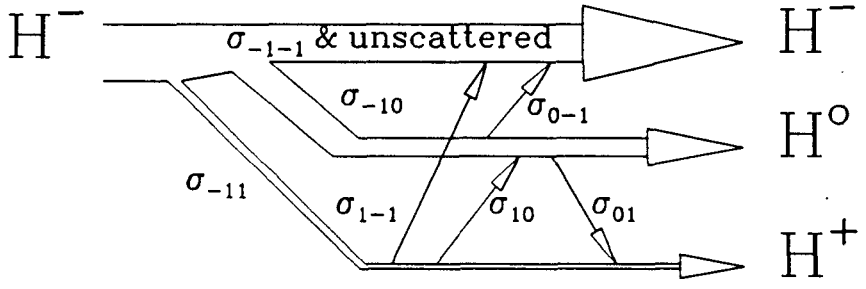

Figure 8. Schematic representation of the various scattering processes in H^- + atom collisions.

The scattered beam fraction F_i is defined to be the background subtracted flux of hydrogen ions or atoms with charge state i divided by the flux of incident H^- ions

$$F_i(\pi) \equiv \frac{[I_i(\pi) - I_i(0)]}{I_{-1}(0)} \tag{1}$$

where i indicates charge–states 0 or 1. For the neutral hydrogen atom (i = 0) beam fraction, $I_0 \boxminus S_0/\gamma$, where S_0 is the measured neutral detector current and γ is the secondary emission coefficient of the neutral detector. A growth curve is obtained by varying the target gas pressure and recording the various ion and atom currents at each target pressure. A typical set of growth curves for F_0 and F_1 and attenuation curve for F_{-1} is shown in Figure 9.

The H° atom and the H^+ fraction growth curve data were fit to quadratic functions of target thickness:

$$F_0 = a_0 + a_1\pi + a_2\pi^2 \tag{2}$$

and

$$F_1 = b_0 + b_1\pi + b_2\pi^2 \tag{3}$$

where the a_i and b_i coefficients are the fit parameters in the analyses. The

constant coefficients a_0 and b_0 were included as fit parameters as an experimental check on the adequacy of the background subtraction of the data prior to analysis. For both F_0 and F_1, the constant coefficients returned from the fits were within one standard deviation of zero thus giving assurance that the backgrounds were adequately subtracted from the data.

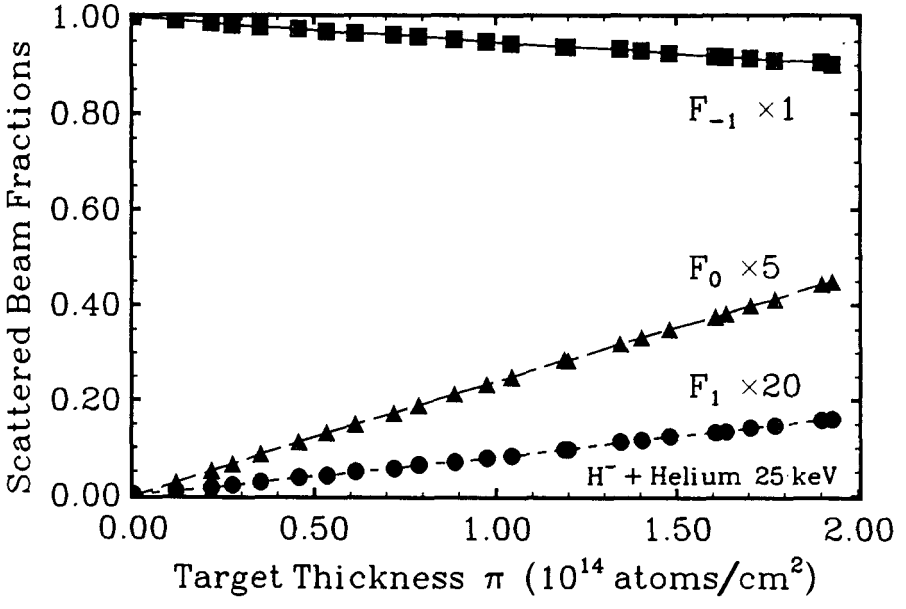

Figure 9. A typical set of growth and attenuation curves.

Assuming a pure incident H^- ion beam and at sufficiently low values of π, the solutions (see, for example, Ref. 5) to the differential equations for growths of the F_0 and F_1 scattered beam fractions are:

$$F_0 = \sigma_{-10}\pi + \tfrac{1}{2}[\sigma_{-11}\sigma_{10} - \sigma_{-10}(\sigma_{-10}+\sigma_{-11}+\sigma_{01}+\sigma_{0-1})]\pi^2 \quad (4)$$

and

$$F_1 = \sigma_{-11}\pi + \tfrac{1}{2}[\sigma_{-10}\sigma_{01} - \sigma_{-11}(\sigma_{-11}+\sigma_{-10}+\sigma_{10}+\sigma_{1-1})]\pi^2 \quad (5)$$

where σ_{ij} is the total cross section for the charge-changing process i→j. The linear coefficients a_1 and b_1 from the growth curve fits are the cross sections for that particular detachment process (σ_{-10} and σ_{-11}, respectively), while the quadratic coefficients a_2 and b_2 are sums of cross section pairs as shown in

Eqs. 4 and 5. Thus for single detachment

$$a_1 = \sigma_{-10}\,; \qquad a_2 = \tfrac{1}{2}[\sigma_{-11}\sigma_{10} - \sigma_{-10}(\sigma_{-10}+\sigma_{-11}+\sigma_{01}+\sigma_{0-1})] \tag{6}$$

and likewise for double detachment

$$b_1 = \sigma_{-11}\,; \qquad b_2 = \tfrac{1}{2}[\sigma_{-10}\sigma_{01} - \sigma_{-11}(\sigma_{-11}+\sigma_{-10}+\sigma_{10}+\sigma_{1-1})]\,. \tag{7}$$

As can be deduced from these equations, non–zero quadratic coefficients are expected. The cross section pair adding positively to the sum in Eq. 6 or 7 ($\sigma_{-11}\sigma_{10}$ or $\sigma_{-10}\sigma_{01}$, respectively) comprising the quadratic coefficient in either case arises from the indirect, two–step process -- the scattering of H^- into the different charge state (H^+ for SED, H^o for DED) followed by a second scattering into the final, correct charge state (H^o for SED, H^+ for DED). The first cross section pair adding negatively to the sum in Eq. 6 or 7 ($\sigma_{-10}\sigma_{-10}$ or $\sigma_{-11}\sigma_{-11}$, respectively) is identical to the quadratic term in the expansion of the exponential ($\exp[-\sigma_{-10}\pi]$ or $\exp[-\sigma_{-11}\pi]$) if one assumes only the direct scattering process. The second cross section pair adding negatively to the sum ($\sigma_{-10}\sigma_{-11}$ or $\sigma_{-11}\sigma_{-10}$) arises from the decrease of the incident H^- beam due to detachment into the other charge state in the first collision and then the remaining H^- beam scattering into the correct charge state from a second collision. The remaining cross section pairs adding negatively to the sum are from scattering into the correct charge state followed by scattering out of it into the two different charge states. As such, the quadratic coefficients hold information about all three hydrogen projectile charge states incident on the target gas even though only H^- was the initial projectile beam. It is emphasized that all of these charge–changing processes listed above are inherent in the scattering of a negative hydrogen ion beam through a gas target -- even under tenuous target gas pressures. A linear fit to the growth curve data is valid only when the cross section pairs comprising the quadratic coefficients sum to zero.

5. TOTAL CROSS SECTIONS

Total cross sections for single- and double-electron detachment (SED or σ_{-10} and DED or σ_{-11}, respectively) in collisions between 3– to 50–keV H^- ions and helium atoms, and collisions of 5– to 50–keV H^- ions with neon and argon atoms have been recently measured with this facility and have been

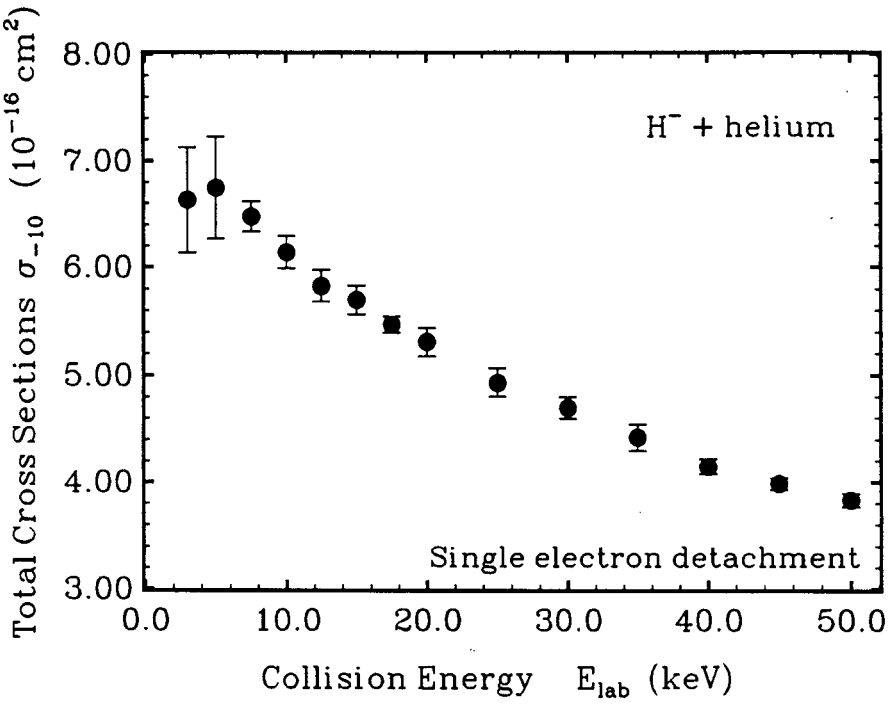

Figure 10. Total cross sections of SED in H^- + helium collisions.

reported [1-5]. As a sample of these results, the total cross sections of single electron detachment in H^- + helium collisions are shown in Figure 10. Previous results have been omitted from this figure for clarity but full comparisons have been made in Refs. 1,3. In general, the agreement of present cross sections with the previous measurements can be explained to a large extent by whether or not the curvature present in the scattered beam growth curves was accounted for in the analysis of the data. For sake of brevity, the reader is referred to those references for specific details concerning these cross sections. All of the necessary experimental parameters were measured, so the reported cross sections here and in Refs. 1,3 are absolute in magnitude. The estimated total systematic uncertainties in the cross sections are 5.7% for σ_{-10} and 3.4% for σ_{-11}. The statistical errors in these data are typically the size of the symbols shown in Figure 10.

6. SUMMARY

An accelerator facility has been constructed for the study of single electron detachment and double electron detachment processes in collisions between 5– to 50–keV H^- ions and atoms and/or molecules. The data from this facility have yielded measurements of SED and DED cross sections, as well as information about some of the other charge–changing processes in the hydrogen – atom (molecule) collision systems. The growths of the H^0 atom and H^+ ion scattered beam fractions as a function of target thickness have nonlinear dependencies on target thickness which are well–described by quadratic functions of the target thickness over the range of target thicknesses used in the present experiments.

7. ACKNOWLEDGEMENTS

The authors are very appreciative of the contributions to this work made by: J.S. Allen, X.D. Fang, A. Sen, and R. Matulioniene. The analyzing magnet support structure was designed by a team of Mechanical Engineering senior students advised by D. Raftopoulos of The University of Toledo. This work is supported by a grant from the Division of Chemical Sciences, Office of Basic Energy Sciences, Office of Energy Research, U.S. Department of Energy.

8. REFERENCES

1. T.J. Kvale,, J.S. Allen, X.D. Fang, A. Sen, and R. Matulioniene, *Phys. Rev.* A **51**, 1351 (1995).
2. T.J. Kvale, J.S. Allen, A. Sen, X.D. Fang, and R. Matulioniene, *Phys. Rev.* A **51**, 1360 (1995).
3. J.S. Allen, X.D. Fang, A. Sen, R. Matulioniene, and T.J. Kvale, *Phys. Rev.* A **52**, 357 (1995).
4. J.S. Allen, X.D. Fang, T.J. Kvale, *Nucl. Instrum. Meth.* B**79**, 106 (1993).
5. T.J. Kvale, A. Sen, and D.G. Seely, "*Electron Detachment in Negative Ion – Atom and Molecule Collisions*," Application of Accelerators in Research and Industry, Proceedings of the Fourteenth International Conference, AIP Conference Proceedings 392, J.L Duggan and I.L. Morgan, ed., AIP Press, p.23-5 (1997).
6. Barnett C.F., Atomic Data for Fusion, Volume 1, "*Collisions of H, H_2, He and Li Atoms and Ions with Atoms and Molecules,*" edited by the Controlled Fusion Atomic Data Center, Publ. ORNL-6086/V1, 1990.

7. Barnett C.F., Ray J.A., Ricci E., Wilker M.I., McDaniel E.W., Thomas E.W., and Gilbody H.B., Atomic Data for Controlled Fusion Research, Volume 1, Physics Division, Oak Ridge National Laboratory, Publ. ORNL-5206/V1, 1977.